Haverford College
Haverford Scholarship

Faculty Publications | Physics

2005

A chiral granular gas

J. C. Tsai

Fangfu Ye

Juan Rodriguez

Jerry P. Gollub
Haverford College, jgollub@haverford.edu

Follow this and additional works at: http://scholarship.haverford.edu/physics_facpubs

Repository Citation
Tsai, J. C., et al. "A chiral granular gas." Phys Rev Lett 94 (2005): 214301.

This Journal Article is brought to you for free and open access by the Physics at Haverford Scholarship. It has been accepted for inclusion in Faculty Publications by an authorized administrator of Haverford Scholarship. For more information, please contact nmedeiro@haverford.edu.

A Chiral Granular Gas

J.-C. Tsai,[1,2] Fangfu Ye,[1] Juan Rodriguez,[2] J. P. Gollub,[1,2] and T. C. Lubensky[1]
[1]*Department of Physics and Astronomy, University of Pennsylvania, Philadelphia, Pennsylvania 19104, USA*
[2]*Department of Physics, Haverford College, Haverford, Pennsylvania 19041, USA*
(Received 6 April 2004; published 31 May 2005)

Inspired by rattleback toys, we created small chiral wires that rotate in a preferred direction on a vertically oscillating platform and quantified their motion with experiment and simulation. We demonstrate experimentally that angular momentum of rotation about particle centers of mass is converted to collective angular momentum of center-of-mass motion in a granular gas of these wires, and we introduce a continuum model that explains our observations.

DOI: 10.1103/PhysRevLett.94.214301 PACS numbers: 45.50.−j, 45.70.−n

There are very few materials to which angular momentum can be delivered uniformly throughout the bulk of a sample. Examples include ferrofluids [1] and liquid crystals [2] in a rotating magnetic field and colloidal dispersions of anisotropic particles illuminated with circularly polarized light [3]. We introduce a two-dimensional (2D) granular gas [4] composed of chiral particles to which angular momentum is delivered by vertical oscillations of the platform on which they lie. The particles of this gas are chiral rods inspired by rattleback toys [5] (elongated objects shaped like the hull of a boat with a curved bottom and a flat top) that have a preferred direction of rotation on a smooth substrate. We show that rotation of particles about their centers of mass, which we call spin, is converted to rotational motion (vorticity) of their centers of mass about the sample center, and we develop a phenomenological theory that explains the observed behavior. Dense 2D granular gases of achiral rods also develop vorticity [6], but of arbitrary sign rather than one fixed by the chirality of constituent particles.

The unusual rotational properties of a rattleback [7] can be traced to a misalignment of the principal axes of its moment inertia tensor relative to the axes of curvature of its curved hull. This misalignment is due to the chiral structure of the rattleback, a fact graphically displayed in the Russian rattleback consisting of a hull with a symmetric bottom and two projections (turtles) on its flat deck whose horizontal orientation can be changed. The configuration with facing turtles is achiral (with C_{2v} symmetry), and that with turtles facing in opposite directions perpendicular to the rattleback's long axis is chiral (with C_2 symmetry). The chiral configuration has a preferred spin direction while the achiral one does not. This suggests that more general chiral objects might behave like rattlebacks and that they might, in particular, have the capacity to convert oscillatory vertical motion into an average rotation in a preferred direction. Motivated by this observation, we created simple chiral objects, with a preferred sense of rotation, that could be produced in sufficient quantities to create a two-dimensional chiral granular gas on a vibrating substrate.

Our chiral particles (generally about a centimeter in length) were each fashioned from a wire segment bent into a configuration with two equal-length arms emerging at right angles from the ends of a central stem, as shown in Fig. 1. The angle α between the two arms is defined in Fig. 1 and can be varied.

We studied the dynamics of individual wires on a flat vertically vibrating platform as a function of arm angle α, root-mean-square (rms) vibration amplitude A, and vibration frequency f. For each driving frequency, the wire starts to spin at or above a lower critical amplitude at which the substrate has an rms acceleration of about $0.98g$, presumably because an initially static wire needs to be accelerated above $1g$ for a substantial fraction of the vibration period in order to become mobile. The sign of average spin is determined by the projection of the upward pointing arm onto the surface as depicted in Fig. 1. All configurations except the planar ones with $\alpha = 0$ or $\alpha = \pi$ are chiral with C_2 symmetry. Figure 2(a) shows that the experimentally measured average angular velocity Ω of the bent wire is a distorted sine function of α with a

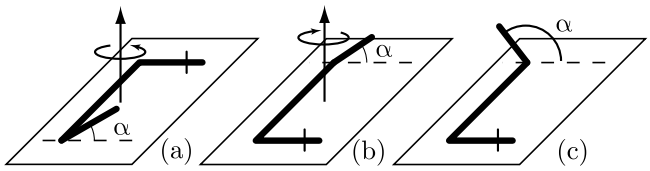

FIG. 1. Schematic representations of bent-wire chiral objects made from a central stem and two arms. (a) Chiral wire with angle $\alpha > 0$, defined as the angle by which the second arm rises out of the plane formed by the stem and first arm (marked with a vertical line). (b) Mirror image of (a), formed by reflection through a plane perpendicular to the central stem, for which the angle α is defined to be negative. In both cases, the curved arrows indicate the direction of spin under vibration. (c) Configuration used in the gas experiments with $\alpha = -3\pi/4$. In general, the spin direction is such that the raised arm moves in the direction of its projection onto the plane of the vibrating surface so that the bent wire in (c) rotates in the counterclockwise direction as seen from above.

 © 2005 The American Physical Society

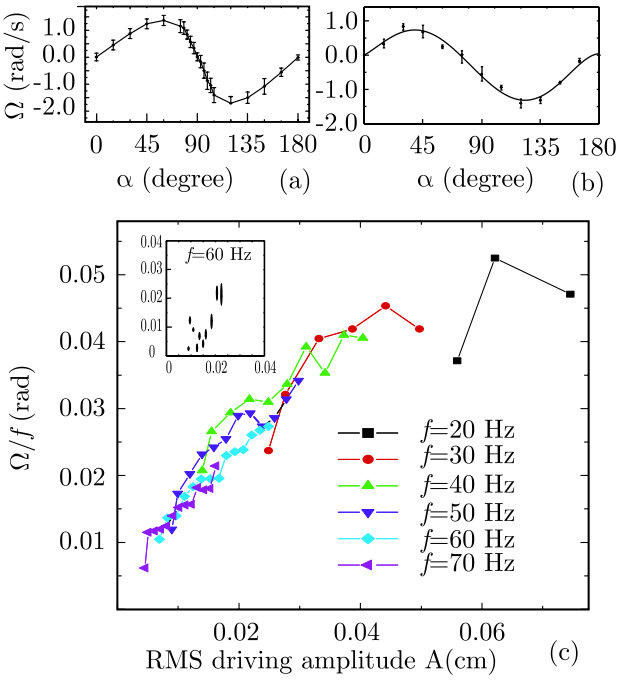

FIG. 2 (color online). (a) Experimental and (b) simulated spin angular velocity Ω as a function of α for $f = 60$ Hz and $A = 3g/(2\pi f)^2$. These curves are repeated periodically for $\alpha < 0$ and $\alpha > \pi$. (c) Plot of experimental scaled spin frequency (Ω/f) for $\alpha = -3\pi/4$ vs vibration amplitude A for different vibration frequencies f. Inset: Ω/f vs A from simulation. In the simulations, $K_n = 500K_0 = 1.25K_t$ and $\gamma_n = 75\gamma_0 = 2.5\gamma_t$, where $K_0 = mg/R_p$ and $\gamma_0 = m\sqrt{g/(10R_p)}$. The simulation error bars reflect both statistical errors and accumulated small numerical errors from each collision.

maximum of about 1.5 rad/s. However, the case $\alpha = \pi/2$ is exceptional, since it is chiral but does not rotate.

Once the vibration amplitude exceeds its frequency-dependent lower critical value $[A \approx 0.98g/(2\pi f)^2]$, the average angle of rotation per vibration, Ω/f, is roughly a unique function that increases with the applied driving amplitude up to the frequency-dependent upper critical amplitude at which the wire first starts to flip over. We observe similar behavior for single wires of different length and find that the lower critical acceleration is approximately independent of length while the upper limit of driving amplitude roughly scales with the length of the wire.

To complement our experimental measurements, we use molecular dynamics to simulate the motion of an individual wire on a vibrating platform. We model our wires with rigidly fixed osculating spheres of radius $R_p = 0.5$ mm. Their stems are constructed from 10 spheres and the arms with from 1 to 4 spheres, but usually with 3 spheres. Each sphere is subjected to the gravitational force $-mg$ in the vertical z direction and to a vertical force f_z and a tangential force $\mathbf{f}_\perp$ arising from its interaction with the platform with oscillating height $h(t) = \sqrt{2}A \sin 2\pi f t$ with $f = 60$ Hz. The latter forces act only if the height of the lowest point on the sphere is less than that of the substrate. Let $\mathbf{r}(t) = [\mathbf{r}_\perp(t), z(t)]$ and $\mathbf{v} = \dot{\mathbf{r}}(t)$ be the position and velocity, respectively, of the center of mass of a given sphere. We model the vertical force as $f_z = -K_n[z - h(t) - R_p] - \gamma_n[v_z - \dot{h}(t)]$, where K_n is a spring constant and γ_n a friction coefficient; and we model the tangential force [8], which allows for an elastic restoring force at the point of contact, as $\mathbf{f}_\perp = -K_t(\mathbf{r}'_\perp - \mathbf{r}_{0\perp}) - \gamma_t \mathbf{v}'_\perp$, where $\mathbf{r}_{0\perp}$ is the tangential position of the point of contact when $z - h(t) - R_p = 0$, $\mathbf{r}'_\perp$ and $\mathbf{v}'_\perp$ are, respectively, the tangential position and velocity of the lowest point of the sphere, K_t is the tangential elastic constant, and γ_t is the tangential friction coefficient. We carried out simulations, using an adaptive Runge-Kutte algorithm, for a range of the parameters, K_n, γ_n, etc. All gave qualitatively similar results provided we chose parameters to yield a small coefficient of restitution—of order 0.2: they all reproduced the observed periodic variation of Ω with angle and increase of Ω with A. In our simulations, the value α_0 of α at which Ω passed through zero varied with arm length, friction coefficients, and amplitude of vibration. Figures 2(b) and 2(c) display our results for a particular set of parameters for which $\alpha_0 \approx 5\pi/12$.

Having established that vertical vibration causes a single chiral wire to rotate, we constructed approximately 400 nearly identical wires with $\alpha = -3\pi/4$. We put these wires in a cylindrical container of radius $R = 6.51$ cm with a flat bottom surface and smooth vertical confining walls. When the container was subjected to oscillatory vertical motion at $f = 20$ to 70 Hz and amplitude between the lower and upper critical values, the wires moved chaotically and dispersed as a uniform-density monolayer gas on the bottom surface. Individual wires in the gas rotated about their centers of mass as they did when isolated but with a much smaller average spin frequency.

Using a fast digital CCD camera, we recorded video images of the granular gas over about 10^4 vibration periods at the rate of one frame every 4 or 8 vibrations and extracted the average velocities $\mathbf{v}$ of the centers of mass of individual particles. This was accomplished by labeling the center of each wire with a fluorescent dot, illuminating with UV "black" light, and using a suitable filter in front of the camera. Figure 3 provides a snapshot of (a) the particles' positions and orientations and (b) their center-of-mass displacements over a 26.6 sec interval. The following qualitative observations follow from this figure and additional observations: (1) velocities increase with distance r from the center, reaching a maximum at the outer boundary; (2) at positions away from the center, the velocities are predominantly in the tangential direction with a nonzero average azimuthal component $v(r) \equiv v_\phi(r)$; (3) the velocity directions are more random near the center; and (4) particles slide along the outer boundary with their long axes parallel to it [9].

To quantify these observations, we measured the average of the angular velocity, $v(r)/r$, of center-of-mass motion

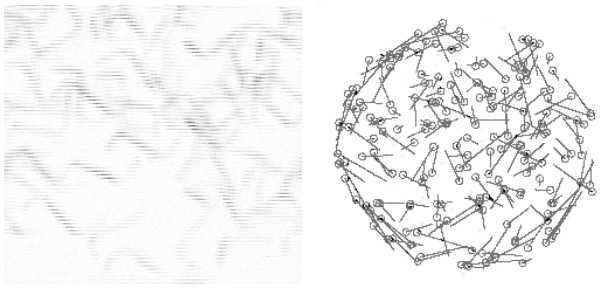

FIG. 3. (a) Still image of $N = 200$ wires in the cell illuminated by visible light. (b) Vectors showing the total displacements of individual particles accumulated for 26.6 sec, with their initial positions marked as circles, for $N = 350$, $f = 60$ Hz, and rms vibrational amplitude $A = 2g/(2\pi f)^2$. In both (a) and (b), arm angle $\alpha = -3\pi/4$, stem length $= 10.0 \pm 0.2$ mm, arm length $= 4.0 \pm 0.2$ mm, and wire diameter $= 0.91 \pm 0.05$ mm.

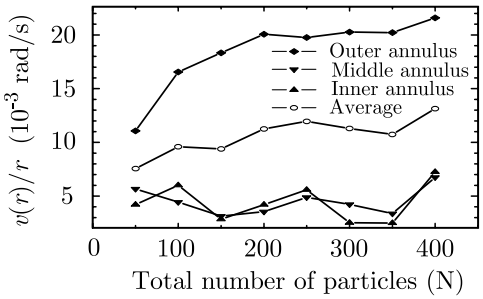

FIG. 4. Measured center-of-mass angular velocity $v(r)/r$ [for $f = 60$ Hz and $A = 2g/(2\pi f)^2$] averaged (to reduce noise) over the three annuli described in the text for different numbers of particles. This angular velocity is greatest in the outer region.

relative to the sample's central axis in three concentric annuli as a function the number N of particles. A small disk of radius $r_0 = 0.65$ cm at the center is excluded and the annuli divide the remaining region $r_0 < r < R$ equally. The results, exhibited in Fig. 4, show that the average angular velocity increases rapidly with increasing r with a value in the outer annulus about 7 times greater than that in the middle annulus for $N > 100$.

We have developed a continuum hydrodynamic theory for our chiral granular gas, which follows earlier theories for isotropic phases of granular gases composed of spherical particles [10] and nematic phases [6,11] composed of rodlike particles. The variables in our theory are fields that are a function of two-dimensional position $\mathbf{x}$ and time t. They are the density $\rho(\mathbf{x}, t)$, the center-of-mass momentum density $\mathbf{g}(\mathbf{x}, t) = \rho\mathbf{v}$ of a standard isotropic fluid, and the spin angular momentum density $l(\mathbf{x}, t) = \mathcal{I}\Omega$ arising from the rotation of particles about their centers of mass, where $\mathcal{I}$ is the moment of inertia density. The density in our experiments is nearly constant, and we assume that the gas is incompressible.

The equation [12] for l is

$$\partial_t l = -\partial_j(l v_j) - \Gamma^\Omega \Omega - \Gamma(\Omega - \omega) + D_\Omega \nabla^2 \Omega + \tau, \quad (1)$$

where $\partial_t \equiv \partial/\partial t$, $\partial_j \equiv \partial/\partial x_j$, and $\omega = (\nabla \times \mathbf{v})_z/2$ is the local collective (or coarse-grained) angular velocity [13], which becomes equal to the angular velocity $v(r)/r$ about the sample center only when the two are independent of r. The first term on the right-hand side of this equation describes the advection of spin angular momentum and the second term friction with the substrate with dissipative coefficient Γ^Ω. The third term, with dissipative coefficient Γ, describes the fact that Ω and ω are equal when the whole sample rotates rigidly and that a rotating system will decay to this state on a frictionless substrate when $\tau = 0$. The fourth term describes diffusion of spin angular momentum with diffusion coefficient D_Ω. The final term τ is the source for spin angular momentum; it is a function of the driving frequency f, amplitude A, and the shape of the particles. This equation predicts an average rotation rate $\Omega = \tau/(\Gamma + \Gamma^\Omega)$ in spatially uniform systems when $\omega = 0$. In the dilute limit, this Ω is the rotation rate of an individual particle.

The momentum equation [12] is

$$\begin{aligned} \partial_t g_i &= -\partial_j(g_i v_j) - \partial_i p + \eta\nabla^2 v_i - \Gamma^v v_i \\ &\quad + \frac{1}{2}\epsilon_{ij}\partial_j\Gamma(\Omega - \omega) \\ &= \partial_j \sigma_{ij} - \Gamma^v v_i, \end{aligned} \quad (2)$$

where σ_{ij} is the stress tensor, p is the pressure, η is the viscosity, Γ^v is a dissipative coefficient, and $\epsilon_{ij} = -\epsilon_{ji}$ the two-dimensional antisymmetric symbol. The first three terms on the right-hand side of this equation are simply the two-dimensional Navier-Stokes equations. The fourth term describes momentum-absorbing friction with the substrate. The final term describes the dissipative interaction between spin and center-of-mass rotation; its form is dictated by the requirement that the sum of center-of-mass and spin angular momenta be conserved when interaction with the substrate described by Γ^Ω, Γ^v, and τ is turned off. Interestingly, Eqs. (1) and (2) also describe equilibrium isotropic films of chiral molecules on a rigid substrate subjected to an external torque. There are additional terms [12] and noise sources that distinguish between equilibrium and nonequilibrium systems that could be included in these equations, but they are not critical to our current treatment.

We seek a steady-state solution to Eqs. (1) and (2) in which the velocity has no radial component and $\Omega(r)$ and the azimuthal component of the velocity $v(r)$ depend only on the distance r from the center. To obtain this solution, we must specify four boundary conditions for the 2 second-order differential equations. The first of these follows from the observation that the particles slide along the outer wall with their long axes parallel to it. This implies that the spin rate about the particles' centers of mass is equal to the angular velocity of the particles about the sample center: $\Omega(R) = v(R)/R$. The second boundary condition at $r = R$ depends on the friction force exerted by the outer wall on particles that collide with it. A friction force proportional

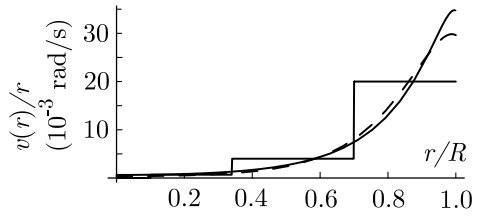

FIG. 5. Plots of $v(r)/r$ for $\lambda_L/R = 0.133$, $\lambda_S/R = 0.025$, and $l/R = 10$ (full line) and for $\lambda_L/R = 0.111$, $\lambda_S/R = 0.00183$, and $l/R = 5$ (dotted curve). Its mean in three bins is shown as discussed in the text. The curves are normalized so that the mean angular velocity in the third bin is equal to the experimentally determined value of 20×10^{-3} rad/s.

to the tangential velocity at the outer wall with a friction coefficient Γ_S imposes the boundary condition $\sigma_{\phi r} = -\Gamma_S v$ on the mixed tangential (ϕ)− radial (r) component of the stress tensor. This is equivalent to the condition $\partial_r v = -l^{-1} v$ on the tangential velocity at $r = R$, where $l^{-1} = [4\Gamma_S - (\Gamma/R)]/(4\eta + \Gamma)$ is an inverse slipping length [14]. The first term in l^{-1}, proportional to Γ_S, is positive and arises directly from friction with the wall. The second term, proportional to Γ/R, is negative and vanishes at $R = \infty$. It arises because an end rather than the center of mass of a rotating particle of length d collides with the wall, experiencing a force in the radial direction that has a tangential component proportional to $d/2R$ at its center of mass. The final boundary conditions are that Ω and ω be nonsingular at the origin.

Introducing lengths via $\lambda_\Omega^2 = D_\Omega/(\Gamma + \Gamma^\Omega)$ and $\lambda_\omega^{-2} = 4\Gamma^v/(4\eta + \Gamma)$ and unitless parameters $a = \Gamma/(\Gamma + \Gamma^\Omega)$ and $b = \Gamma/(4\eta + \Gamma)$, we can write Eqs. (2) and (3) in the steady-state limit as

$$(\lambda_\Omega^2 \nabla^2 - 1)\Omega + a\omega = -\tau/(\Gamma + \Gamma^\Omega) \quad (3a)$$

$$(\nabla^2 - \lambda_\omega^{-2})\omega - b\nabla^2\Omega = 0. \quad (3b)$$

When Ω and ω depend only on r, the exact solutions to Eqs. (3) are linear combinations of $I_0(r/\lambda_L)$ and $I_0(r/\lambda_S)$ where I_0 is the Bessel function of imaginary argument and $\lambda_{S,L}^{-2} = [c \pm \sqrt{c^2 - 4s^2}]/(2\lambda_\Omega^2)$, where $s = \lambda_\Omega/\lambda_\omega$ and $c = 1 - ab + s^2$. The velocity is then $v(r) = A[I_1(r/\lambda_L) + \beta(\lambda_L/R, \lambda_S/R, l/R) I_1(r/\lambda_S)]$, where the coefficients A and β can easily be calculated from the boundary conditions.

Our experiments on collective motion provide only two reliable data points: the average of the angular velocity $v(r)/r$ in the outer two annuli. Our expression for $v(r)$ has four undetermined parameters [15]: λ_L/R, λ_S/R, l/R, and the amplitude A. Thus, there should be a two-dimensional manifold of theoretical curves that fit the data. We show two of these curves in Fig. 5. While it would be ideal to improve the measurement statistics and to calculate dissipative coefficients from kinetic theory, these are difficult tasks, and the present comparison does show that collective rotation can be understood in a consistent way.

We have demonstrated that particle chirality induces individual spin and collective angular momentum in two-dimensional granular gases. Related phenomena should occur both in three-dimensional homochiral granular systems and in granular systems of net chirality zero but composed of particles of opposite chirality. In addition, our model should apply with minor modifications to colloidal and other equilibrium systems such as those studied in Ref. [3].

This work was supported in part by the National Science Foundation under Grants No. DMR04-04670 (F. Y., T. C. L.) and No. DMR04-05187 (J. P. G.), and No. DMR00-79909 (J. C. T.). We are grateful to Tadeshi Tokieda for introducing us to the wonderful world of Russian rattlebacks.

[1] J. C. Bacri, A. Cebers, and R. Perzynski, Phys. Rev. Lett. **72**, 2705 (1994).

[2] Kalman B. Migler and Robert B. Meyer, Phys. Rev. Lett. **66**, 1485 (1991); T. Frisch, S. Rica, P. Coullet, and J. M. Gilli, Phys. Rev. Lett. **72**, 1471 (1994).

[3] Z. Cheng, P. M. Chaikin, and T. G. Mason, Phys. Rev. Lett. **89**, 108303 (2002).

[4] I. Goldhirsch, Annu. Rev. Fluid Mech. **35**, 267 (2003).

[5] J. Walker, Sci. Am. **172**, No. 10, 241 (1979).

[6] Daniel L. Blair, T. Neicu, and A. Kudrolli, Phys. Rev. E **67**, 031303 (2003); Igor S. Aranson and Lev S. Tsimring, Phys. Rev. E **67**, 021305 (2003).

[7] G. Walker, Quart. J. Pure and Appl. Math. **28**, 175 (1896); H. Bondi, Proc. R. Soc. London, Ser. A **405**, 265 (1986); A. Garcia and M. Hubbard, Proc. R. Soc. London, Ser. A **418**, 165 (1988).

[8] Leonardo E. Silbert, D. Ertas, G. S. Grest, T. C. Halsey, D. Levine, and S. J. Plimpton, Phys. Rev. E **64**, 051302 (2001). When $|\mathbf{f}_\perp| > \mu|f_z|$, we replace $\mathbf{f}_\perp$ with $-\mu|f_z|\mathbf{v}_t/|\mathbf{v}_t|$ where $\mu = 0.7$ is the dynamic friction coefficient.

[9] Videos of the collective motion may be viewed at http://www.haverford.edu/physics-astro/Gollub/chiral.

[10] C. Bizon, M. D. Shattuck, J. B. Swift, and H. L. Swinney, Phys. Rev. E **60**, 4340 (1999).

[11] S. Ramaswamy, R. A. Simha, and J. Toner, Europhys. Lett. **62**, 196 (2003).

[12] Strictly speaking, in the nonequilibrium incompressible system lacking Galilean invariance that we are considering, $-\partial_j(lv_j)$ in Eq. (1) and $-\partial_j(g_i v_j)$ in Eq. (2), should be replaced, respectively, by $-bv_i\partial_i l$ and by $-a_1\rho v_j\partial_j v_i - a_2\partial_i v^2$, where b, a_1, and a_2 are constants. These replacements do not change our results. See John Toner and Yuhai Tu, Phys. Rev. E **58**, 4828 (1998).

[13] This angular velocity is half of the vorticity $(\nabla \times \mathbf{v})_z$ of fluid mechanics. See, e.g., L. D. Landau and E. M. Liftshitz, *Fluid Mechanics* (Pergamon, Oxford, 1959).

[14] J. L. Barrat and L. Bocquet, Phys. Rev. Lett. **82**, 4671 (1999).

[15] The speed $v(r)$ depends only on the product ab. Measurements of $\Omega(r)$ are needed to determine a and b separately.